

Title: Cycloastragenol improves hepatic steatosis by activating farnesoid X receptor signalling

Authors: Ming Gu, Shiyong Zhang, Yuanyuan Zhao, Jinwen Huang, Yahui Wang, Yin Li, Shengjie Fan, Li Yang, Guang Ji, Qingchun Tong, Cheng Huang



PII: S1043-6618(16)31358-5
DOI: <http://dx.doi.org/doi:10.1016/j.phrs.2017.04.021>
Reference: YPHRS 3572

To appear in: *Pharmacological Research*

Received date: 16-12-2016
Revised date: 16-3-2017
Accepted date: 14-4-2017

Please cite this article as: Gu Ming, Zhang Shiyong, Zhao Yuanyuan, Huang Jinwen, Wang Yahui, Li Yin, Fan Shengjie, Yang Li, Ji Guang, Tong Qingchun, Huang Cheng. Cycloastragenol improves hepatic steatosis by activating farnesoid X receptor signalling. *Pharmacological Research* <http://dx.doi.org/10.1016/j.phrs.2017.04.021>

This is a PDF file of an unedited manuscript that has been accepted for publication. As a service to our customers we are providing this early version of the manuscript. The manuscript will undergo copyediting, typesetting, and review of the resulting proof before it is published in its final form. Please note that during the production process errors may be discovered which could affect the content, and all legal disclaimers that apply to the journal pertain.

Cycloastragenol improves hepatic steatosis by activating farnesoid X receptor
signalling

Ming Gu¹, Shiyong Zhang¹, Yuanyuan Zhao¹, Jinwen Huang², Yahui Wang¹, Yin Li¹,
Shengjie Fan^{1,3}, Li Yang⁴, Guang Ji⁵, Qingchun Tong^{3*} and Cheng Huang^{1*}

1 School of Pharmacy, Shanghai University of Traditional Chinese Medicine,
Shanghai, China

2 School of Chemical and Environmental Engineering, Shanghai Institute of
Technology, Shanghai, China

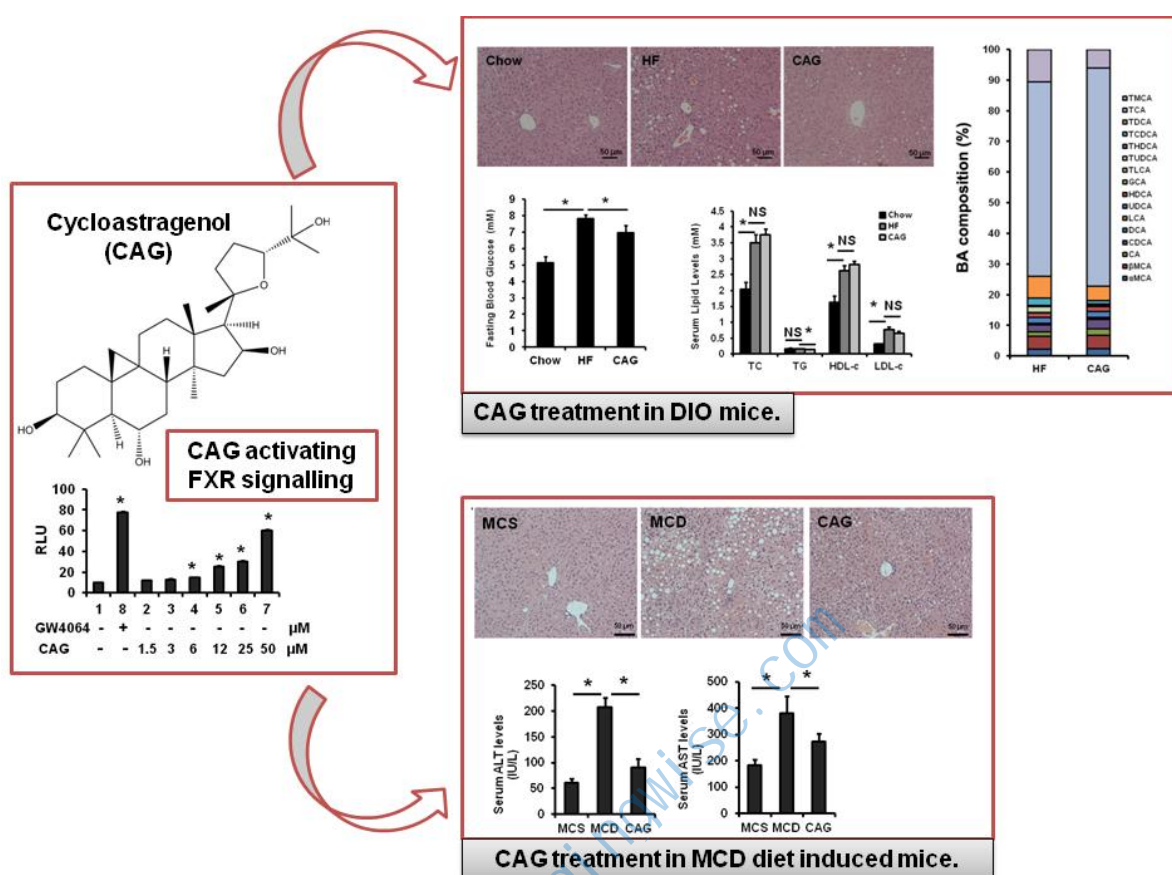
3 Brown Foundation Institute of Molecular Medicine and Program in Neuroscience,
Graduate School of Biological Sciences, University of Texas McGovern Medical
School, Houston, TX, USA

4 Research Center for Traditional Chinese Medicine of Complexity Systems,
Shanghai University of Traditional Chinese Medicine, Shanghai, China

5 Institute of Digestive Disease, Longhua Hospital, Shanghai University of
Traditional Chinese Medicine, Shanghai, China

*Correspondence: Guang Ji, jiliver@vip.sina.com; Qingchun Tong,
Qingchun.Tong@uth.tmc.edu; Cheng Huang, chuang@shutcm.edu.cn

Graphical Abstract



1. Cycloastragenol stimulated FXR transcription activity.
2. Cycloastragenol lowered blood glucose, serum triglyceride in DIO mice.
3. Cycloastragenol alleviated hepatic steatosis in DIO and MCD mice.

Abstract

Non-alcoholic fatty liver disease (NAFLD) has become a global health problem. However, there is no approved therapy for NAFLD. Farnesoid X receptor (FXR) is a potential drug target for treatment of NAFLD. In an attempt to screen FXR agonists, we found that cycloastragenol (CAG), a natural occurring compound in *Astragali Radix*, stimulated FXR transcription activity. In animal studies, we demonstrated that CAG treatment resulted in obvious reduction of high-fat diet induced lipid accumulation in liver accompanied by lowered blood glucose, serum triglyceride levels and hepatic bile acid pool size. The stimulation of FXR signalling by CAG treatment in DIO mice was confirmed via gene expression and western blot analysis. Molecular docking data further supported the interaction of CAG and FXR. In addition, CAG alleviated hepatic steatosis in methionine and choline deficient L-amino acid diet (MCD) induced non-alcoholic steatohepatitis (NASH) mice. Our data suggest that CAG ameliorates NAFLD via the enhancement of FXR signalling.

Key words: cycloastragenol; metabolic syndrome; non-alcoholic fatty liver disease; farnesyl X receptor

Abbreviations

ALT, alanine aminotransferase; AST, aspartate transaminase; BA, bile acid; DIO, diet-induced obesity; CA, cholic acid; DMSO, dimethylsulfoxide; FXR, farnesyl X receptor; HDL-c, high density lipoprotein cholesterol; HF, high-fat; IPITT, intraperitoneal insulin tolerance test; LDL-c, low density lipoprotein cholesterol; NAFLD, non-alcoholic fatty liver disease; NASH, non-alcoholic steatohepatitis; NF- κ B, nuclear factor kappa B; NR, nuclear receptor; MS, metabolic disease; Rosi, rosiglitazone; TBA, total bile acid; TC, total cholesterol; TCA, taurocholic acid; TCDCA, tauro-chenodeoxycholic acid; TG, triglyceride; TUDCA, tauro-ursodeoxycholic acid

Introduction

Non-alcoholic fatty liver disease (NAFLD) is the most common liver metabolic disease encompassing a spectrum of medical condition, from hepatic steatosis to non-alcoholic steatohepatitis (NASH) followed by progression to fibrosis, cirrhosis and hepatocellular carcinoma. NAFLD is often accompanied by multifaceted metabolic disorder factors including obesity, insulin resistance, dyslipidemia and etc [1, 2]. Due to the prevalence of over-nutritious lifestyle, concealed disease progression, and eruptible obesity morbidity, NAFLD has been a leading killer worldwide [3, 4]. Although many attempts were made to find an appropriate molecule target and related chemical drug to treat NAFLD, there is no therapy approved for NAFLD currently [5].

Farnesoid X receptor (FXR) is a ligand-activated nuclear receptor transcription factor which serves as an intracellular bile acid sensor in enterohepatic system [6]. FXR plays roles in correcting multiple metabolic disorders including cholestasis, dyslipidaemia, IR, inflammation, NAFLD via regulating a series of genes expression [7-11]. On the other hand, loss of FXR in mice lead to development of impaired glucose tolerance and insulin resistance, elevated circulating lipids levels and severe liver steatosis [12, 13]. Obeticholic acid (OCA), a lipophilic bile acid derivative and a potent FXR activator, has been the focal point in drug research field due to its significantly beneficial effects on NAFLD in both animal experiments and human trials [14-16]. Thus, FXR activation is a potential therapeutic approach for NAFLD.

Astragali Radix, the roots of *Astragalus membranaceus (Fisch) Bunge*, is widely distributed in Europe and Asia [17, 18]. In China, Astragali Radix has been used as an herbal medicine to treat various diseases such as diabetes, hyperlipidemia, atherosclerosis and cancers [19-21]. Astragaloside IV, the major constituent of Astragali Radix, has been identified to be mostly responsible for the effect observed with Astragali Radix [17, 18, 22]. However, astragaloside IV is metabolized as cycloastragenol (CAG) mostly [23], which is also natural occurred in Astragali Radix

[22]. Recently CAG has been demonstrated to activate telomerase and shown potential pharmacological effects including anti-aging, anti-oxidation, relieving endoplasmic reticulum (ER) stress and etc [23-26]. However, whether CAG could act on controlling MS and NAFLD remains elusive.

In screening for FXR agonists from natural compounds, we found that CAG stimulated the FXR transcription activities. Here we aim to reveal whether CAG treatment improves liver steatosis and other metabolic disorders.

Methods

Chemicals and diets

Cycloastragenol (Pusi Biotech, Chengdu, China) and Ursodeoxycholic Acid (UDCA, Zhongxin Biotech, Tianjin, China) were dissolved in dimethylsulfoxide (DMSO) to the final concentration of 50 mM for cell culture. GW4064, T090173, Rosiglitazone (Rosi), int-777, WY14643, rifampicin, and bile acid standard references were purchased from Sigma–Aldrich (St. Louis, MO, USA). High-fat diets (HF, 60% of calories derived from fat), Chow diets (Chow, 10% of calories derived from fat) were purchased from Research Diet (D12492 and D12450B, New Brunswick, NJ, USA). Methionine and choline deficient L-amino acid diets (MCD, 20% of calories derived from fat) and methionine and choline supplement diet (MCS) were purchased from Qifa Biol Comp (A02082002B and A02082003B, Shanghai, China).

Cell culture and FXR deletion HepG2 cell

HepG2 (ATCC) cells were seeded on six-well plates (1×10^6 cells/well) and grown to 80% confluence with high-glucose DMEM containing 10% FBS at 37°C in 5% CO₂. The following day, cells were treated with vehicle control, CAG (25 μM). After 24-hour treatment, the cells were collected for RNA isolation.

To generate the FXR deletion cell, HepG2 cells were transfected with pX330-U6-Chimeric_BB-CBh-hSpCas9 containing a single-guiding nucleotide sequence (Forward sequence: taggtaacaaagaagccccgcat, reverse sequence:

aaacatgctggggcttctttgta) for targeting human FXR for 48 hours. Then, cells were treated with vehicle or CAG (25 μ M). After 24-hour treatment, the cells were collected for RNA analysis.

Gene reporter assays

The reporter assay was performed using the Dual-Luciferase Reporter Assay System (Promega, USA) as previously described [27]. For nuclear receptor transcription activity assay, the expression plasmids for phFXR, phRXR and FXR-response reporter (EcRE-LUC), pCMXGal-hPPAR α , γ , LXR α , β , and PXR -LBD and the Gal4 reporter vector MH100 \times 4-TK-Luc were co-transfected with a reporter construct so that 1 μ g of the relevant plasmid combined with 1 μ g of reporter plasmids and 0.1 μ g of pREP7 (*Renilla luciferase*) reporter could be used to normalize transfection efficiencies. The transfection mixture, which contained 10 μ g of total plasmids and 15 μ l FuGENE-HD (Roche) per ml of DMEM, was added to HEK293T cells (ATCC) for 24 h and then removed. The FXR, PPAR α , PPAR γ , LXRs, and PXR agonists (GW4064, WY14643, Rosiglitazone, T090173 and Rifampicin respectively), CAG were added to fresh media and the cells were incubated for another 24 h to determine luciferase activity.

Animal experiment

All animal protocols used in this study were approved by Shanghai University of Traditional Chinese Medicine (Approval Number: SZY20150522). Female C57BL/6 mice were purchased from the SLAC Laboratory (Shanghai, China). Animals were housed and bred according to standardized procedures, under controlled temperature (22–23°C) and on a 12-h light, 12-h dark cycle. Six-week-old female mice were fed with high-fat diet for 12 weeks to induce obesity and these mice were then randomly divided into four groups according to body weight: Chow group (10% of calories derived from fat), High-fat group (HF, 60% of calories derived from fat), UDCA group (HF diet supplemented with UDCA powder (Ursofalk, Losan Pharma GmbH, Germany), at dose of 80 mg/100 g diet) and CAG group (HF diet supplemented with

CAG powder, at dose of 100 mg/100 g diet). Mice were treated for additional 6 weeks. Food intake amount was measured by recording food weight every two days throughout the experiment. The amount of food intake over a 24-hour period was calculated.

For MCD-diet fed animals experiment, female C57BL/6 mice were managed as the same methods in HF diet-fed experiment. Six-week-old female mice randomly divided into three groups according to body weight: MCS group (fed MCS diet), MCD (fed MCD diet), and CAG group (MCD diet supplemented with CAG powder at 100 mg/100 g diet). Mice were fed with corresponding diets for additional 6 weeks before the experiment ending.

Intraperitoneal glucose tolerance and insulin tolerance tests

At the end of the HF-diet treatment, mice were fasted overnight (12 h). The baseline glucose values (0 min), prior to the injection of glucose (1 g/kg body weight), were measured through tail vein. Additional blood samples were collected at regular intervals (15, 30, 60, and 90 min) during glucose tolerance tests.

Serum chemistry analysis

At the end of animal experiment study, mice were anesthetized 20% urethane (Sigma, St. Louis, MO) and cardiac blood was taken. Serum alanine aminotransferase (ALT), aspartate transaminase (AST), triglyceride (TG), total cholesterol (TC), HDL cholesterol (HDL-c), and LDL cholesterol (LDL-c) were measured using a Hitachi 7020 Automatic Analyzer (Hitachi, Ltd., Tokyo, Japan) with 100 μ l of heart blood serum.

Histochemistry

Liver tissues were fixed in formalin, and paraffin-embedded sections were cut at 5 μ m. Sections were stained with haematoxylin and eosin according to a standard procedure. For Oil red O staining, the frozen liver tissues were embedded in O.C.T. compound (Sakura Finetek, Torrance, CA), sliced, and then stained with Oil red O.

Hepatic lipid content Analysis

Lipid content was measured as described [28]. Briefly, 100 mg of the liver tissue was homogenized with 2 ml chloroform-methanol and then agitated overnight on an orbital shaker at 4°C. The homogenate was then centrifuged (5 min at 2,300 g), 0.9% NaCl solution was subsequently added to the liquid phase before the samples were vortexed. Phase separation was induced by centrifugation (800 g for 10 min), and the bottom phase was removed to a new tube and evaporated to dryness, Samples were then resuspended in 500 µl chloroform-1% Triton X-100, evaporated to dryness, and finally resuspended in 500 µl of water. The quantities of total cholesterol and triglycerides (KINGHA WK, China) in liver lipid extracts were then assayed by using enzymatic kits according to the manufacturers' protocols.

Quantitative PCR

Total RNA from HepG2 cells, mouse livers and small intestines was isolated using the TRIzol method (Invitrogen, Carlsbad, CA). The first-strand cDNA was synthesized with a cDNA synthesis kit (Fermentas, Madison, WI). Quantitative real-time polymerase chain reaction (PCR) was carried out using SYBR green PCR Mastermix. The results were analysed on an ABI StepOnePlus real-time PCR system (Applied Biosystems, USA). Values were normalized to β -actin. Sequences for primers are listed in Table 1 and 2.

Western blotting

HepG2 (ATCC) cells were seeded on six-well plates (1×10^6 cells/well) and grown to 80% confluence with high-glucose DMEM containing 10% FBS at 37°C in 5% CO₂. The cells were treated with 0.1% DMSO (Mock), UDCA (25 µM) CAG (12, 25 and 50 µM) for 24-hours, then the cells were collected for protein extracting. Whole-cell lysates were prepared using RIPA buffer (Beyotime Biotechnology, Shanghai, China), followed by separated by 10% SDS-PAGE and transferred to nitrocellulose membranes. The membranes were probed with antibodies specific for CYP7A1 (Millipore, Billerica, CA, USA), β -ACTIN, CYP8B1, ABCC2, NR0B2 (Santa Cruz

Inc., Santa Cruz, CA, USA), CPT1 α (Abcam, Cambridge, MA, USA). Immunoreactive proteins were visualized using LI-COR Odyssey Infrared Imaging System (LI-COR Biosciences, Lincoln, Nebraska, USA), according to the manufacturer's instructions. The relative protein levels were normalized to β -ACTIN.

Quantification of bile acids in mice

Measurements of total bile acids (TBA) in mouse livers and faeces were performed as the following. Livers were weighed and homogenized in 10 X volume water. TBA levels of homogenate samples were measured by the TBA Measurement Kit (KeHua, China) after quantification of intracellular protein concentration. The TBA levels were normalized to intracellular protein content. Protein concentrations were determined by BCA protein assay kit (Sigma, St. Louis, MO). The faecal TBA analysis was performed as the same method described above and calculated by normalizing the faeces weight.

To measure hepatic BA pool size and composition, liver-tissue samples were weighed, and TBA was extracted in 5X volumes of acetonitrile followed by centrifugation at 14,300 rpm for 10 min. The supernatant was dried under nitrogen steam before re-dissolved in methanol solution (methanol:water:formic acid = 50:50:0.01) and then subject to centrifugation at 14,300 rpm for 10 min. Supernatant bile salt species were analysed by ultra-performance liquid chromatography (UPLC) triple time of flight/MS analysis (UPLC-MS, Waters Co., MA, USA). The relevant parameters were described in a previous publication [29].

Molecular docking

The crystal structure of FXR (PDB code 1OT7) was retrieved from the Research Collaboratory for Structural Bioinformatics (RCSB) protein data bank. CAG was constructed using the sketcher module in Sybyl and their minimum energy conformations were calculated using the Minimize module of Sybyl. The force field was Tripos with an 8 Å cutoff for non-bonded interactions, and the atomic point charges were also calculated with Gasteiger-Huckel. Minimizations were achieved

using the steepest descent method for the first 100 steps, followed by the Broyden-Fletcher-Goldfarb-Shanno (BFGS) method until the root-mean-square (RMS) of the gradient became <0.005 kcal/(mol·Å). The Surflex-Dock module implemented in the Sybyl program was used for the docking studies. The obeticholic acid binding pocket of FXR was used for the docking simulation. CAG were docked into the binding site by an empirical scoring function and a patented search engine in Surflex-Dock, applied with the automatic docking. Other parameters were established by default in the software.

Statistical analysis

All values were expressed as means \pm SEM and analysed using the statistical package for the social science (SPSS, version 15.0). Paired or unpaired two tailed t-tests were used to detect difference in the mean values of treatment group and control and analysis of variance (ANOVA) for the difference among more than two groups. Differences with P values < 0.05 were considered to be statistically significant.

Results

CAG stimulates FXR transactivity *in vitro*

To test whether CAG (Figure 1 A) is able to activate FXR, we performed a gene reporter assay by co-transfected hFXR, hRXR expression vectors and FXR-dependent reporter (EcRE-LUC) into HEK293T cells. The results demonstrated that CAG activated the FXR transactivity in a dose-dependent manner (Figure 1B). FXR agonists have been shown to activate a series of target genes. We therefore examined whether CAG could regulate known FXR target gene expression in HepG2 cells. As expected, CAG treatment markedly regulated the expression of FXR target gene NR0B2, ABCC2, CYP7A1, PPAR α and PPAR α downstream gene CPT1 α when compared with mock control groups (Fig. 1C-D). Then, we deleted FXR gene in HepG2 cells using CAS9 technique. The genes regulation directed by CAG-treatment was blunted largely in FXR deletion cells (Fig. 1E-F). Next, the change of FXR signalling was further confirmed by western blot analysis (Fig. 1G-H).. Taken

together, our data suggest that CAG may regulate FXR transactivity.

We also analysed the effects of CAG on other important nuclear receptor transactivity. The results showed that there were no effects of CAG on PXR, PPAR γ , β/δ and LXR α , β transactivities (data not shown) and PPAR α transactivity (Figure 1I), suggesting that the CAG selectively activates FXR.

TGR5, a bile acid sensitive G-protein coupled receptor, has been reported to bind with diverse FXR agonists [30]. To clarify whether CAG also activate TGR5-cAMP signalling, we transiently transfected hTGR5 expression plasmid and pCRE-Luc reporter into HEK293T cells over a period of 24 h. Even with a high dose (CAG at 50 μ M), CAG stimulation showed no obvious response on the pCRE-Luc reporter signalling (data not shown), indicating that CAG have limited influence on activating hTGR5.

CAG interacts with FXR

To further assay the potential direct interaction between CAG and FXR, the structure of the complex of FXR and CAG was analysed by molecular docking. The obeticholic acid binding site of FXR has been validated as the binding pocket of CAG. CAG was docked into the binding pocket, the pose that ranked first complex with FXR was shown in (Figures 2A). CAG skeleton was surrounded by a hydrophobic pocket composed of Met262, Leu284, Met287, Ala288, His291, Met325, Arg328, Ser329, Ile332, Leu345, Ile354, Tyr358, Met362, Tyr366, Met447, Tyr451 and Trp466, where van der Waals forces play a dominant role in the interactions. These interactions were postulated to be the primary reason for CAG activity. The specific interaction of CAG with FXR is also displayed in (Figures 2B).

CAG improves metabolic profiles in diet-induced obesity (DIO) mice

To test whether CAG affects body-weight, blood glucose and lipid levels in DIO mice, obese C57BL/6 mice fed HFD were divided in two groups, one was continuously fed on a high-fat (HF) diet as control and the another was fed the same HF diet mixed with CAG (100 mg CAG/100 g diet) for additional 6 weeks. CAG treatment did not

obviously change body weight gain (Figure 3A) or food intake (Figure 3B), but lowered fasting blood glucose (Figure 3C), although the glucose intolerance was not improved (Figure 3D), suggesting that CAG may improve fasting glucose homeostasis in DIO mice.

We next assayed the lipid profile in the mice. As expected, HF diet feeding elevated serum TC, HDL-c and LDL-c levels compared to chow controls (Figure 3E), and notably, CAG treatment decreased serum TG levels in DIO mice (Figure 3E), but not TC, HDL-c and LDL-c.

CAG ameliorates hepatic steatosis in DIO mice

OCA, UDCA and other FXR agonists have been reported to have therapeutic effects against NAFD and NASH [11, 15, 31, 32]. We therefore determined whether CAG could improve hepatic steatosis. By comparing the HE staining results among HF, UDCA and CAG-treated mice liver sections, we found that CAG treatment significantly reduce hepatic steatosis (Figure 4A), and this was confirmed by lipid content measurement, which showed notably decrease in TG, but not TC, contents when compared to HF-fed controls (Figure 4B and C). Although several previous reports showed that UDCA has therapeutic effects on fatty liver disease [31, 32], we observed that UDCA did not significantly reduced TG levels in livers of DIO mouse (Figure 4A, B and C). Serum ALT and AST levels were markedly higher in DIO mice compared to those in the chow diet control mice, but there was no difference in ALT or AST levels between DIO controls, UDCA-treated and CAG-treated mice (Figure 4D and E). These results indicate that CAG may ameliorate lipid accumulation in liver of DIO mice.

CAG alters BA composition *in vivo*

The main physiological function of FXR is to maintain BA homeostasis [33]. Therefore, total bile acids in livers and faeces were determined following analysis of hepatic BA composition. After CAG treatment, DIO mice showed markedly decreased TBA levels in livers but no change in faeces, compared with HF controls (Fig. 5B and

C). Meanwhile, the composition of hepatic BA was also altered by CAG treatment. In contrast to high fat diet fed mice, CAG treatment strikingly decreased the fraction of murine taurocholic acid (TMCA), tauro-chenodeoxycholic acid (TCDCA) and tauro-deoxycholic acid (TDCA), which was accompanied with an increased fraction of the β murine taurocholic acid (β MCA), chenodeoxycholic acid (CDCA) and cholic acid (CA) in CAG-treated DIO mice (Fig. 5A and Table 3).

CAG activates FXR signal *in vivo*

To further clarify the FXR agonise effect of CAG *in vivo*. We analysed expression levels of nuclear receptors (Figure 6A), the FXR downstream genes involved in bile acid metabolism (Figure 6B), lipid and glucose metabolism (Figure 6C) in the liver tissue of CAG-treated mice. The results showed that CAG treatment significantly increased *Nr0b2*, *Osta*, *Cyp3a11*, *Akr1b7*, *Pgc1 β* , *Cpt1a*, *Acox1* and decreased *Cyp7a1*, *Cyp8b1*, *Pck1*, *G6pc*, *Scd1* mRNA levels in DIO mice livers (Figure 6A-C). Recently, the activation of intestinal FXR has been shown to reduce body fat and improve metabolic disorders [34]. So we assayed the mRNA level of the FXR target gene in intestine of the mice. The results showed that CAG elevated intestinal *Nr0b2* and *Osta* expression levels in DIO mice (Figure 6D). Furthermore, CAG also lowered the expression of inflammatory genes *Mcp1*, *Il1 β* , *Il6* in the liver of CAG groups in contrast to those in HF groups (Figure 6E), suggesting that CAG may activate FXR signalling and feedback loops *in vivo*, improve liver lipid metabolism signalling and block inflammation process in DIO mice.

CAG corrects liver lipid metabolic dysfunction in MCD diet-induced mice

Next, we tested the anti-hepatic steatosis effect of CAG on NASH induced by MCD diet feeding. C57BL/6 mice fed MCD were divided in two groups, one continued to feed a MCD diet as control and the other fed MCD diet mixed with CAG (100 mg CAG/100 g diet). After 6 weeks of treatment, we found the liver steatosis in MCD controls was obviously severer than those in MCS control mice, and CAG-treatment attenuated the steatosis, evident from the HE staining results (Figure 7A). Oil red O

staining confirmed that the lipid accumulation was decreased in the liver of CAG treated MCD mice (Figure 7A). Furthermore, hepatic lipid content and serum liver functional measurements also demonstrated astonishingly higher hepatic lipid contents (Figure 7B and C), serum ALT and AST levels in MCD group mice in contrast to MCS, and CAG treatment lowered the ALT and AST levels (Figure 7D and E). These results indicate that CAG treatment effectively reverses MCD diet induced NAFLD and impairment in liver function in C57BL/6 mice.

Gene expression experiments showed that a series of genes such as *Pgc1a*, *Cpt1a*, and *Cpt1b*, were markedly increased while *Il1b*, *Il6* and *Cd68* were decreased in the CAG treatment groups compared to MCD controls (Fig. 7F and G). Collectively, these data suggest that CAG treatment may change the expression of genes involved in fatty acid metabolism and inflammation response.

Discussion

Here, we found CAG, a natural molecule isolated from Astragali Radix activated nuclear receptor FXR signalling *in vivo* and *in vitro*. We further confirmed the pharmacological effect of CAG on treating metabolic syndrome, especially ameliorating NAFLD in DIO and MCD-induced mice. These effects were probably achieved via the stimulation of FXR signalling. Our data raise the possibility to use CAG as a novel natural FXR agonist that can effectively treat NAFLD.

Previous studies examined astragaloside IV as a main active compound from Astragali Radix exerting relevant therapeutic roles [18, 21, 35, 36]. CAG, the derivative of astragaloside IV is another abundant chemical existing in Astragali Radix [25, 37]. However, the pharmacological effect and molecular mechanism of CAG on preventing MS are largely unknown. FXR is regarded as an energy metabolism adapter [33, 38]. Activation of FXR leading to ameliorating lipid and glucose metabolism has received a particularly intense attention [8, 11]. To explore whether CAG has a potential correlation to FXR and possesses anti-MS activity, we utilized FXR gene reporter assay to analyse the influence of CAG treatment on FXR

transactivity *in vitro*. As expected, FXR gene reporter assay revealed that CAG apparently activated FXR reporter signal in a dose dependent manner, which was proved by the change of mRNA and protein levels of FXR downstream target genes in HepG2 cells, including increased expressions of *NR0B2*, *FGF19*, *ABCC2*, *APOC2* and *PPAR α* , but decreased expression of *CYP7A1*, but such effects were largely blunted or reversed in condition of FXR deletion. These data were also supported by the molecular docking result that showed CAG may interact with FXR directly and enhance the FXR transactivity. These results suggest that CAG is a potential agonist of FXR.

Astragali Radix and astragaloside IV have been shown effectively improve lipid metabolism and attenuates serum triglyceride content *in vivo* [19, 20, 36]. Similarly, we also found CAG treatment effectively lowered HF diet-induced fasting plasm blood glucose and triglyceride levels without changing the bodyweight and food intake in DIO mice. These data showed CAG treatment is beneficial to the treatment against hyperlipidemia and hyperglycemia, which similar to Astragali Radix and astragaloside IV. It suggests that glucose-lipid lowering effects of CAG may be related to the activation of FXR in DIO mice.

FXR agonists have been proven to treat NAFLD effectively. It prompted our interest on whether CAG-supplement could ameliorate hepatic steatosis in DIO mice. Excitingly, we observed a significant improvement of the morphology in the liver of DIO mice fed CAG, while UDCA-treatment showed a less therapeutic effect on steatosis in DIO mice at indicated dose, although several groups reported its effects on fatty liver disease. The subsequent liver lipids contents analysis also confirmed this finding, suggesting that CAG may attenuate microvesicular steatosis in the mice and play a more active role in NAFLD than UDCA.

FXR is a key modulator of bile acid metabolism in the enterohepatic system that acts via various feed forward and feedback loops. FXR deficiency impairs bile acid homeostasis [33, 39]. After a 6-week treatment, the hepatic TBA levels in CAG-treated mice were lowered. In addition, decreased proportions of TMCA,

TCDCA and TDCA with increased fraction of β mTCA CA and CDCA in CAG-treated mice showed an altered hepatic BA composition. Hepatic *Osta*, *Cyp3a11*, *Cyp7a1* and *Cyp8b1* are essential for BA release, BA detoxification, controls BA synthesis and BA hydroxylation [33], which regulated by FXR. Consistent with the characteristics of reported FXR agonists, CAG markedly increased *Osta*, *Cyp3a11* while reduced *Cyp7a1* and *Cyp8b1* gene expression levels in DIO mice, indicating that CAG is able to activate the BA loop of FXR signalling in liver tissue of the mice. This finding further hints that CAG may be a natural FXR modulator and influences BA homeostasis.

A series of FXR target genes which are highly expressed in enterohepatic systemliver and consist of a complex FXR signal network. We found CAG-treatment markedly induced the mRNA expression of liver *Nr0b2* which is the most direct target gene of and engages a feedback loop that repressing *Cyp7A1* and *Cyp8b1*, resulting in inhibition of bile acid synthesis [33, 39]. Meanwhile, CAG significantly enhanced *Apoc2*, *Akr1b7*, but reduced *Pck1*, *G6pc* and *Scd1* genes expression which are regulated by FXR and involved in hepatic gluconeogenesis and lipogenesis [33]. We also found CAG largely elevated intestinal FXR target gene mRNA levels in DIO mice, such as *Nr0b2* and *Osta*, indicating intestinal stimulation of FXR signalling by CAG may play a role in improving MS. These results further supports the altered hepatic BA pools and metabolism signal pathway and partly explained the lowered blood glucose and TG levels in DIO mice of CAG-treatment group. This finding is consistent with the action of other FXR agonists reported *in vitro*.

NASH is considered as a worsened stage of steatosis and characterized by ballooning steatosis, inflammation, and degeneration of hepatocytes function [2]. To extend our findings on diet-induced steatosis models, we used a MCD-diet induced mouse NASH model to test the impact of CAG treatment on severe hepatic steatosis. Excitingly, CAG treatment also potently blocked hepatic lipid accumulation in MCD-diet induced mice according to HE staining and lipid content determination. Hepatic steatosis is often accompanied with hepatocyte inflammation responses. FXR agonist has been

reported to activate anti-inflammation [9, 10, 40]. Previously, Both Astragali Radix and astragaloside IV are reported to alleviate inflammatory via inhibiting NF- κ B activity [24, 41-43]. In the present study, we found the unchanged NF- κ B activity by CAG-treating *in vitro*, but reduced liver inflammation factor expression *in vivo*. Gene expression analysis demonstrated CAG treatment strikingly reduced *Mcp1*, *Il1 β* , *Il6* and *Mcp1*, *Il1 β* , *Il6*, *Cd68* mRNA levels respectively in DIO and MCD-induced mice, suggesting that CAG-treatment reduces liver inflammation progress is independent on the inhibiting NF- κ B activity.

Fatty acid β oxidation, mainly mediated by *Ppara/Pgc1/Acox1/Cpt1* signalling, plays an important role in promoting lipids consumption and ameliorating steatosis in hepatocyte [38, 44]. FXR agonists were indeed reported to be able to enhance hepatic *Ppara* mediated mitochondrial fatty acid β -oxidation and TG clearance [38, 45, 46]. We found that the effect of CAG on increasing *PPAR α* and *CPT1 α* mRNA levels was blocked under FXR deleted cell, although CAG did not directly activate *PPAR α* transactivity. Similarly, CAG treatment also remarkably increased liver *Pgc1*, *Acox1* and *Cpt1* expressions in DIO and MCD-diet induced mice. It indicates that CAG may stimulate *Ppara/Pgc1/Acox1/Cpt1* signalling and promote β oxidation in the liver which partly explained its therapeutic effect on hepatic steatosis. These findings further manifests that CAG is a natural FXR signal activator.

One complicating factor in the study of FXR biology is that bile acids are also ligands for multiple other receptors controlling MS [30, 40]. Our data from reporter assays suggest that it is unlikely that CAG activates several important BA-related receptors such as *PPAR α* , γ , *LXR α* , β , *PXR* and *TGR5*. However, we found that CAG elevated the proportions of β -mTCA CA and CDCA *in vivo*, which are endogenous ligands for *TGR5*, indicating that endogenous *TGR5* activation by bile acids might mediate partial CAG therapeutic effects.

In conclusion, we found that CAG stimulated FXR transactivity signalling *in vitro* and *in vivo*. CAG supplementation not only corrected hyperglycaemia, hyperlipidaemia and reconstituted the bile acid pool in DIO mice, but also ameliorated hepatic steatosis

and inflammation progress in DIO and MCD-diet fed mice. Our data suggest that the effects of CAG on metabolic disorder is mediated by FXR activation.

Competing interests: The authors declare no conflict of interest.

Author contributions

M.G., L.Y., Q.T. G.J. and C.H. conceived the experiments. M.G., S.Z., Y.Z., Y.W., S.F., J.H. and Ying. L. performed the experiments, M.G. and C.H. analysed the data. All authors discussed the results and commented on the manuscript. M.G. Q.T. and C.H wrote the manuscript.

www.counteragingscience.com

References

- [1] R.J. Perry, V.T. Samuel, K.F. Petersen, G.I. Shulman, The role of hepatic lipids in hepatic insulin resistance and type 2 diabetes, *Nature*. 510 (2014) 84-91.
- [2] M.E. Rinella, Nonalcoholic fatty liver disease: a systematic review, *Jama*. 313 (2015) 2263-2273.
- [3] S. Traussnigg, C. Kienbacher, E. Halilbasic, C. Rechling, L. Kazemi-Shirazi, H. Hofer, P. Munda, M. Trauner, Challenges and Management of Liver Cirrhosis: Practical Issues in the Therapy of Patients with Cirrhosis due to NAFLD and NASH, *Dig Dis*. 33 (2015) 598-607.
- [4] R.J. Wong, M. Aguilar, R. Cheung, R.B. Perumpail, S.A. Harrison, Z.M. Younossi, A. Ahmed, Nonalcoholic steatohepatitis is the second leading etiology of liver disease among adults awaiting liver transplantation in the United States, *Gastroenterology*. 148 (2015) 547-555.
- [5] G. Musso, M. Cassader, R. Gambino, Non-alcoholic steatohepatitis: emerging molecular targets and therapeutic strategies, *Drug Discov*. 15 (2016) 249-274.
- [6] D.J. Parks, S.G. Blanchard, R.K. Bledsoe, G. Chandra, T.G. Consler, S.A. Kliewer, J.B. Stimmel, T.M. Willson, A.M. Zavacki, D.D. Moore, J.M. Lehmann, Bile acids: natural ligands for an orphan nuclear receptor, *Science*. 284 (1999) 1365-1368.
- [7] Y. Zhang, P.A. Edwards, FXR signaling in metabolic disease, *FEBS Lett*. 582 (2008) 10-18.
- [8] Y. Zhang, F.Y. Lee, G. Barrera, H. Lee, C. Vales, F.J. Gonzalez, T.M. Willson, P.A. Edwards, Activation of the nuclear receptor FXR improves hyperglycemia and hyperlipidemia in diabetic mice, *PNAS*. 103 (2006) 1006-1011.
- [9] L. Adorini, M. Pruzanski, D. Shapiro, Farnesoid X receptor targeting to treat nonalcoholic steatohepatitis, *Drug Discov Today*. 17 (2012) 988-997.
- [10] R.M. Gadaleta, K.J. van Erpecum, B. Oldenburg, E.C. Willemsen, W. Renooij, S. Murzilli, L.W. Klomp, P.D. Siersema, M.E. Schipper, S. Danese, G. Penna, G. Laverny, L. Adorini, A. Moschetta, S.W. van Mil, Farnesoid X receptor activation inhibits inflammation and preserves the intestinal barrier in inflammatory bowel disease, *Gut*. 60 (2011) 463-472.

- [11] Y. Ma, Y. Huang, L. Yan, M. Gao, D. Liu, Synthetic FXR agonist GW4064 prevents diet-induced hepatic steatosis and insulin resistance, *Pharm Res.* 30 (2013) 1447-1457.
- [12] B. Kong, J.P. Luyendyk, O. Tawfik, G.L. Guo, Farnesoid X receptor deficiency induces nonalcoholic steatohepatitis in low-density lipoprotein receptor-knockout mice fed a high-fat diet, *J Pharmacol Exp Ther.* 328 (2009) 116-122.
- [13] P. Lefebvre, B. Staels, Failing FXR expression in the liver links aging to hepatic steatosis, *J Hepatol.* 60 (2014) 689-690.
- [14] B.A. Neuschwander-Tetri, R. Loomba, A.J. Sanyal, J.E. Lavine, M.L. Van Natta, M.F. Abdelmalek, N. Chalasani, S. Dasarthy, A.M. Diehl, B. Hameed, K.V. Kowdley, A. McCullough, N. Terrault, J.M. Clark, J. Tonascia, E.M. Brunt, D.E. Kleiner, E. Doo, Farnesoid X nuclear receptor ligand obeticholic acid for non-cirrhotic, non-alcoholic steatohepatitis (FLINT): a multicentre, randomised, placebo-controlled trial, *Lancet.* 385 (2015) 956-965.
- [15] G. Musso, Obeticholic acid and resveratrol in nonalcoholic fatty liver disease: all that is gold does not glitter, not all those who wander are lost, *Hepatology.* 61 (2015) 2104-2106.
- [16] L. Verbeke, I. Mannaerts, R. Schierwagen, O. Govaere, S. Klein, I. Vander Elst, P. Windmolders, R. Farre, M. Wenes, M. Mazzone, F. Nevens, L.A. van Grunsven, J. Trebicka, W. Laleman, FXR agonist obeticholic acid reduces hepatic inflammation and fibrosis in a rat model of toxic cirrhosis, *Sci Rep.* 6 (2016) 33453.
- [17] T.T. Dong, K.J. Zhao, Q.T. Gao, Z.N. Ji, T.T. Zhu, J. Li, R. Duan, A.W. Cheung, K.W. Tsim, Chemical and biological assessment of a chinese herbal decoction containing Radix Astragali and Radix Angelicae Sinensis: Determination of drug ratio in having optimized properties, *J Agr Food Chem.* 54 (2006) 2767-2774.
- [18] W. Zhang, C. Zhang, R. Liu, H. Li, J. Zhang, C. Mao, C. Chen, Quantitative determination of Astragaloside IV, a natural product with cardioprotective activity, in plasma, urine and other biological samples by HPLC coupled with tandem mass spectrometry, *J Chromatogr B.* 822 (2005) 170-177.
- [19] Y. Long, X.X. Zhang, T. Chen, Y. Gao, H.M. Tian, Radix Astragali Improves Dysregulated

Triglyceride Metabolism and Attenuates Macrophage Infiltration in Adipose Tissue in High-Fat Diet-Induced Obese Male Rats through Activating mTORC1-PPAR gamma Signaling Pathway, *PPAR Res.* 2014 (2014) 189085.

[20] S. Ren, H. Zhang, Y. Mu, M. Sun, P. Liu, Pharmacological effects of Astragaloside IV: a literature review, *J Tradit Chin Med.* 33 (2013) 413-416.

[21] N. Zhang, X.H. Wang, S.L. Mao, F. Zhao, Astragaloside IV improves metabolic syndrome and endothelium dysfunction in fructose-fed rats, *Molecules.* 16 (2011) 3896-3907.

[22] A. Movafeghi, D. Djozan, J.A. Razeghi, T. Baheri, Identification of volatile organic compounds in leaves, roots and gum of *Astragalus compactus* Lam. using solid phase microextraction followed by GC-MS analysis, *Nat Prod Res.* 24 (2010) 703-709.

[23] P.K. Ma, B.H. Wei, Y.L. Cao, Q. Miao, N. Chen, C.E. Guo, H.Y. Chen, Y.J. Zhang, Pharmacokinetics, metabolism, and excretion of cycloastragenol, a potent telomerase activator in rats, *Xenobiotica.* (2016) 1-12.

[24] Y. Zhao, Q. Li, W. Zhao, J. Li, Y. Sun, K. Liu, B. Liu, N. Zhang, Astragaloside IV and cycloastragenol are equally effective in inhibition of endoplasmic reticulum stress-associated TXNIP/NLRP3 inflammasome activation in the endothelium, *J Ethnopharmacol.* 169 (2015) 210-218.

[25] S. Wang, C. Zhai, Q. Liu, X. Wang, Z. Ren, Y. Zhang, Q. Wu, S. Sun, S. Li, Y. Qiao, Cycloastragenol, a triterpene aglycone derived from *Radix astragali*, suppresses the accumulation of cytoplasmic lipid droplet in 3T3-L1 adipocytes, *Biochem Bioph Res Co.* 450 (2014) 306-311.

[26] D. Gui, Y. Guo, F. Wang, W. Liu, J. Chen, Y. Chen, J. Huang, N. Wang, Astragaloside IV, a novel antioxidant, prevents glucose-induced podocyte apoptosis in vitro and in vivo, *Plos One.* 7 (2012) e39824.

[27] C. Huang, Y. Zhang, Z. Gong, X. Sheng, Z. Li, W. Zhang, Y. Qin, Berberine inhibits 3T3-L1 adipocyte differentiation through the PPARgamma pathway, *Biochem Bioph Res Co.* 348 (2006) 571-578.

[28] J. Folch, M. Lees, G.H. Sloane Stanley, A simple method for the isolation and purification of

total lipides from animal tissues, *J Biol Chem.* 226 (1957) 497-509.

[29] F. Yang, Y. Xu, A. Xiong, Y. He, L. Yang, Y.J. Wan, Z. Wang, Evaluation of the protective effect of Rhei Radix et Rhizoma against alpha-naphthylisothiocyanate induced liver injury based on metabolic profile of bile acids, *J Ethnopharmacol.* 144 (2012) 599-604.

[30] Y. Kawamata, R. Fujii, M. Hosoya, M. Harada, H. Yoshida, M. Miwa, S. Fukusumi, Y. Habata, T. Itoh, Y. Shintani, S. Hinuma, Y. Fujisawa, M. Fujino, A G protein-coupled receptor responsive to bile acids, *J Biol Chem.* 278 (2003) 9435-9440.

[31] A. Pathil, J. Mueller, A. Warth, W. Chamulitrat, W. Stremmel, Ursodeoxycholyll lysophosphatidylethanolamide improves steatosis and inflammation in murine models of nonalcoholic fatty liver disease, *Hepatology.* 55 (2012) 1369-1378.

[32] V. Ratziu, V. de Ledinghen, F. Oberti, P. Mathurin, C. Wartelle-Bladou, C. Renou, P. Sogni, M. Maynard, D. Larrey, L. Serfaty, D. Bonnefont-Rousselot, J.P. Bastard, M. Riviere, J. Spenard, A randomized controlled trial of high-dose ursodesoxycholic acid for nonalcoholic steatohepatitis, *J Hepatol.* 54 (2011) 1011-1019.

[33] T. Matsubara, F. Li, F.J. Gonzalez, FXR signaling in the enterohepatic system, *Mol Cell Endocrinol.* 368 (2013) 17-29.

[34] S. Fang, J.M. Suh, S.M. Reilly, E. Yu, O. Osborn, D. Lackey, E. Yoshihara, A. Perino, S. Jacinto, Y. Lukasheva, A.R. Atkins, A. Khvat, B. Schnabl, R.T. Yu, D.A. Brenner, S. Coulter, C. Liddle, K. Schoonjans, J.M. Olefsky, A.R. Saltiel, M. Downes, R.M. Evans, Intestinal FXR agonism promotes adipose tissue browning and reduces obesity and insulin resistance, *Nat Med.* 21 (2015) 159-165.

[35] R.N. Zhou, Y.L. Song, J.Q. Ruan, Y.T. Wang, R. Yan, Pharmacokinetic evidence on the contribution of intestinal bacterial conversion to beneficial effects of astragaloside IV, a marker compound of astragali radix, in traditional oral use of the herb, *Drug Metab Pharmacok.* 27 (2012) 586-597.

[36] H. Wu, Y. Gao, H.L. Shi, L.Y. Qin, F. Huang, Y.Y. Lan, B.B. Zhang, Z.B. Hu, X.J. Wu, Astragaloside IV improves lipid metabolism in obese mice by alleviation of leptin resistance and

regulation of thermogenic network, *Sci Rep.* 6 (2016) 30190.

[37] L.Y. Yung, W.S. Lam, M.K. Ho, Y. Hu, F.C. Ip, H. Pang, A.C. Chin, C.B. Harley, N.Y. Ip, Y.H. Wong, Astragaloside IV and cycloastragenol stimulate the phosphorylation of extracellular signal-regulated protein kinase in multiple cell types, *Planta Med.* 78 (2012) 115-121.

[38] L. Rui, Energy metabolism in the liver, *Compr Physiol.* 4 (2014) 177-197.

[39] T.T. Lu, M. Makishima, J.J. Repa, K. Schoonjans, T.A. Kerr, J. Auwerx, D.J. Mangelsdorf, Molecular basis for feedback regulation of bile acid synthesis by nuclear receptors, *Mol Cell.* 6 (2000) 507-515.

[40] M. Arrese, S.J. Karpen, Nuclear receptors, inflammation, and liver disease: insights for cholestatic and fatty liver diseases, *Clin Pharmacol Ther.* 87 (2010) 473-478.

[41] W.J. Zhang, B. Frei, Astragaloside IV inhibits NF- κ B activation and inflammatory gene expression in LPS-treated mice, *Mediat Inflamm.* 2015 (2015) 274314.

[42] M. Ryu, E.H. Kim, M. Chun, S. Kang, B. Shim, Y.B. Yu, G. Jeong, J.S. Lee, Astragali Radix elicits anti-inflammation via activation of MKP-1, concomitant with attenuation of p38 and Erk, *J Ethnopharmacol.* 115 (2008) 184-193.

[43] P.K. Lai, J.Y. Chan, L. Cheng, C.P. Lau, S.Q. Han, P.C. Leung, K.P. Fung, C.B. Lau, Isolation of anti-inflammatory fractions and compounds from the root of *Astragalus membranaceus*, *Phytother Res.* 27 (2013) 581-587.

[44] A.P. Jensen-Urstad, C.F. Semenkovich, Fatty acid synthase and liver triglyceride metabolism: housekeeper or messenger?, *Biochim Biophys Acta.* 1821 (2012) 747-753.

[45] I. Pineda Torra, T. Claudel, C. Duval, V. Kosykh, J.C. Fruchart, B. Staels, Bile acids induce the expression of the human peroxisome proliferator-activated receptor alpha gene via activation of the farnesoid X receptor, *Mol Endocrinol.* 17 (2003) 259-272.

[46] B. Cariou, B. Staels, FXR: a promising target for the metabolic syndrome?, *Trends Pharmacol Sci.* 28 (2007) 236-243.

Figure and Figure legends

Figure 1. Cycloastragenol activates FXR transactivity *in vitro*. (A) Structure of Cycloastragenol. (B) FXR transactivity. HEK293T cells were co-transfected with phFXR, phRXR expression plasmids and FXR-dependent reporter (EcRE-LUC) for 24 h and treated with the FXR agonist GW4064 (5 μ M), control (DMSO), Cycloastragenol (1.5, 3, 6, 12, 25, 50 μ M) for another 24 h. The relative luciferase activities (RLU) were measured by comparison to renilla luciferase activities. (C - F) The relative gene expression levels in CAG-treated (25 μ M) and control (DMSO) HepG2 cells with or without FXR deletion. β -ACTIN was used as an internal control for normalizing the mRNA levels. (G) The western blotting image in CAG-treated (12, 25 and 50 μ M), UDCA-treated (25 μ M) and Mock control (DMSO) HepG2 cells. The relative quantification data of western blotting (H). (I) PPAR α transactivity. HEK293T cells were co-transfected with pCMX-PPAR α -LBD-Gal4, MH100 \times 4-TK-Luc expression plasmids for 24 h and treated with the PPAR α agonist WY14643 (10 μ M), control (DMSO) and Cycloastragenol (50 μ M) for another 24 h. The relative luciferase activities (RLU) were measured by comparison to renilla luciferase activities. The results represent three independent experiments, and data are presented as means \pm SEM. (n = 3). * P < 0.05 vs. HEK293T or HepG2 control.

Figure 2. Cycloastragenol Interacts with FXR. (A) the structure of the complex of FXR and Cycloastragenol. (B) Cycloastragenol skeleton.

Figure 3. Cycloastragenol improves glucose-lipid homeostasis in diet-induced obesity (DIO) C57BL/6 mice. (A) Body weight during the 6-week treatment. (B) Food intake amount. (C) Fasting blood glucose level. (D) Intraperitoneally glucose tolerance test (IPGTT). The mice were fasted overnight, and glucose were intraperitoneally injected (1 g of /kg body weight) and blood glucose levels were determined at the indicated time points. (E) Serum total cholesterol (TC), triglyceride (TG), low-density lipoprotein cholesterol (LDL-c), high-density lipoprotein cholesterol (HDL-c) levels. Data are presented as means \pm SEM (n = 7). *P < 0.05, vs.

Chow or HF group, NS: No significance.

Figure 4. Cycloastragenol ameliorates hepatic steatosis in DIO mice. (A) H&E staining of liver sections ($\times 200$). (B) Liver TG level. (C) Liver TC level. (D) Serum ALT level. (E) Serum AST level. Data are presented as means \pm SEM (n = 7). *P < 0.05, vs. Chow or HF group, NS: No significance.

Figure 5. Cycloastragenol alters BA composition in DIO mice. (A) Hepatic BA composition. (B) Hepatic TBA level. (C) Fecal TBA level. Data are presented as means \pm SEM (n = 7). *P < 0.05, vs. HF group, NS: No significance.

Figure 6. Cycloastragenol regulates FXR signal and alleviates the inflammation in DIO mice liver. The mRNA levels of hepatic nuclear receptors (A), hepatic bile acids metabolism related genes (B), hepatic glucose and lipid metabolism related genes (C), FXR target genes in intestine (D), and inflammation related genes (E). *β -actin* was used as an internal control for normalizing the mRNA levels. Data are presented as means \pm SEM (n = 6). *P < 0.05, vs. HF group.

Figure 7. Cycloastragenol inhibits lipid accumulation in liver of MCD-diet induced NASH mice. (A) H&E and Oil-red O staining of liver sections ($\times 200$). (B) Liver TG level. (C) Liver TC level. (D) Serum ALT level. (E) Serum AST level. Data are presented as means \pm SEM (n = 7). *P < 0.05, vs. MCS or MCD group, NS: No significance. (F and G) The relative gene expression levels in livers from CAG-treated and MCD control mice. *β -Actin* was used as an internal control for normalizing the mRNA levels. Data are presented as means \pm SEM (n = 6). *P < 0.05, vs. MCD group.

Table 1. Sequences of the human primers used in real time PCR

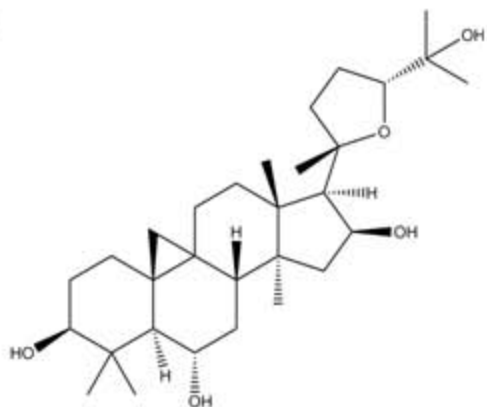
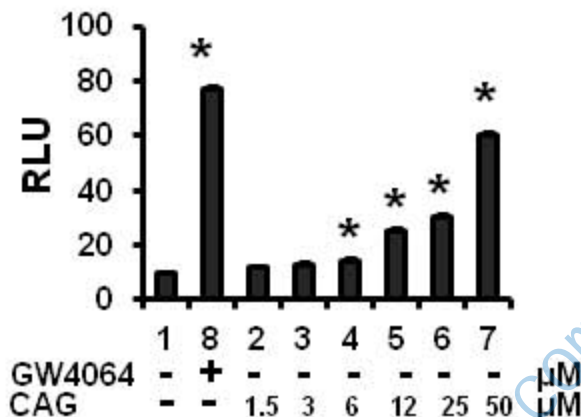
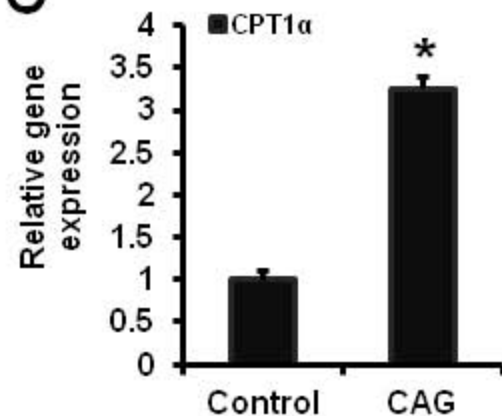
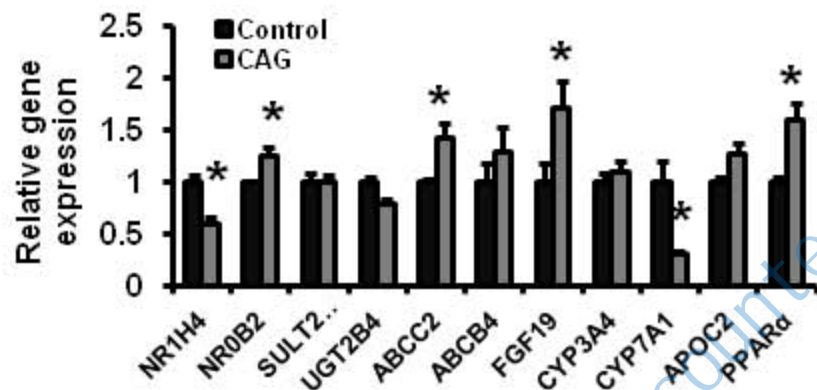
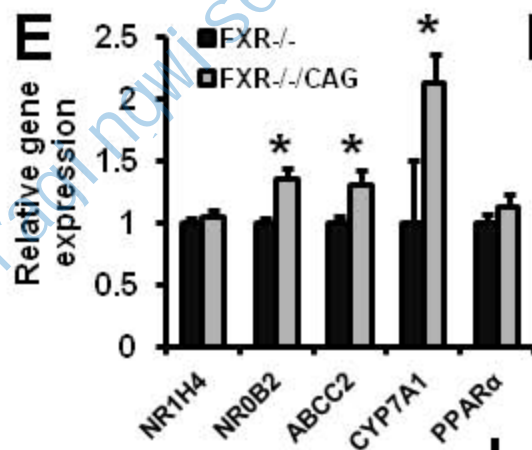
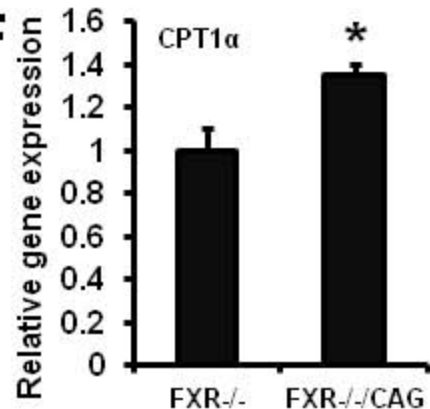
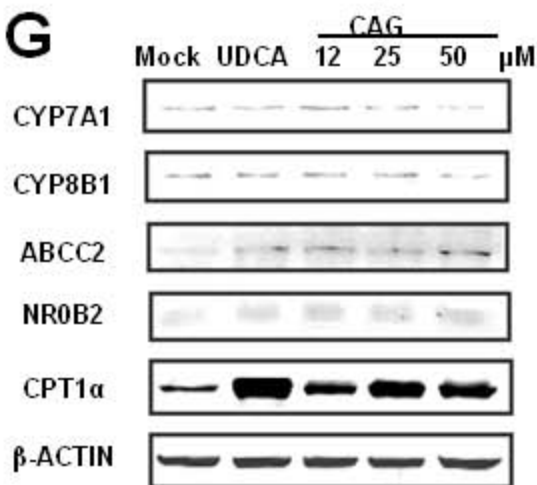
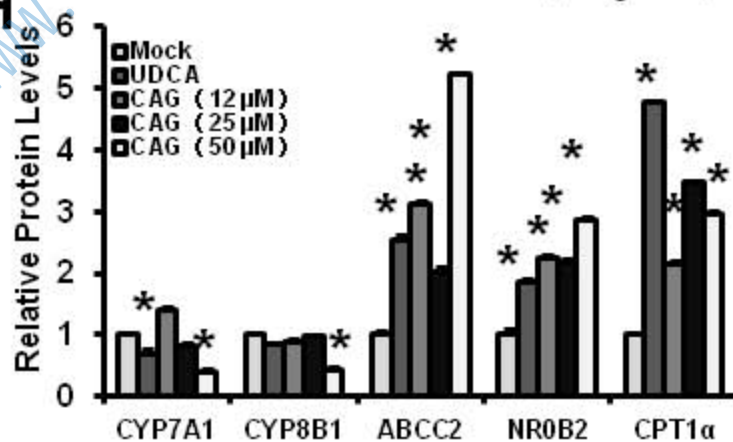
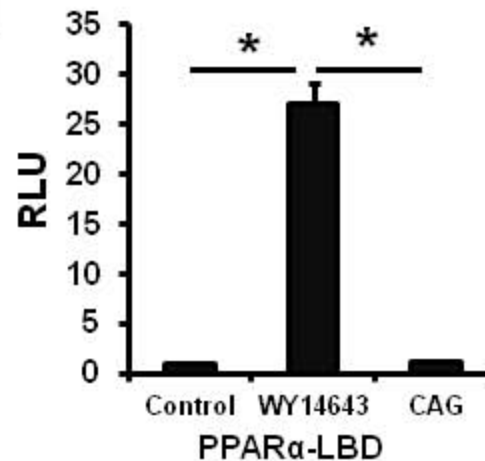
Gene	Sense primer	Anti-sense primer
<i>NR1H4</i>	ATGGGAATGTTGGCTGAATG	CCTGCATGACTTTGTTGTCG
<i>NR0B2</i>	AGGCCTCCAAGCCGCCTCCCACATTGGGC	GCAGGCTGGTCGGAAACTTGAGGGT
<i>UGT2B4</i>	CCTATGTGCCTGTTGTTATGTCA	AACATTTGGTAAGAGTGGGTGAG
<i>SULT2A1</i>	AACAGGACACAGGAAGAACCAT	CAGTCCCCAGATACACCTTTTC
<i>ABCC2</i>	TCGGAATGTGAATAGCCTGAAG	CGCAAGGATGATGAAGAATATCG
<i>ABCB4</i>	GCAGACGGTGGCCCTGGTTGG	TGGAAAACAGCACCGGCTCCTG
<i>APOC2</i>	GAGATGCCTAGCCCGACCTTCCTCAC	GCTCAGTCTGAACCTGGGGGATCAGG
<i>CYP7A1</i>	GAGAAGGCAAACGGGTGAAC	AGCACAGCCCAGGTATGGA
<i>CYP8B1</i>	CCCTCTTCCCTACCTCTCAGT	AAGTGTGTGACCATAAGCAGGA
<i>PPARα</i>	GAAATGGGAAACATCCAAGAGA	CACAGGATAAGTCACCGAGGA
<i>CYP3A4</i>	AGTGGAAAACCTCAAGGAGATGG	CGATGTTCACTCCAAATGATGT
<i>CPT1α</i>	TGGCGTCTGAGAAGCATCAGCATA	ACACCACGTAAAGGCAGAAGAGGT
<i>FGF19</i>	CACGGGCTCTCCAGCTGCTTCCTGCG	TCTCCTCGAAAGCACAGTCTTCCTCCG
<i>β-ACTIN</i>	AATCTGGCACACACCTTCTA	ATAGCACAGCCTGGATAGCAAC

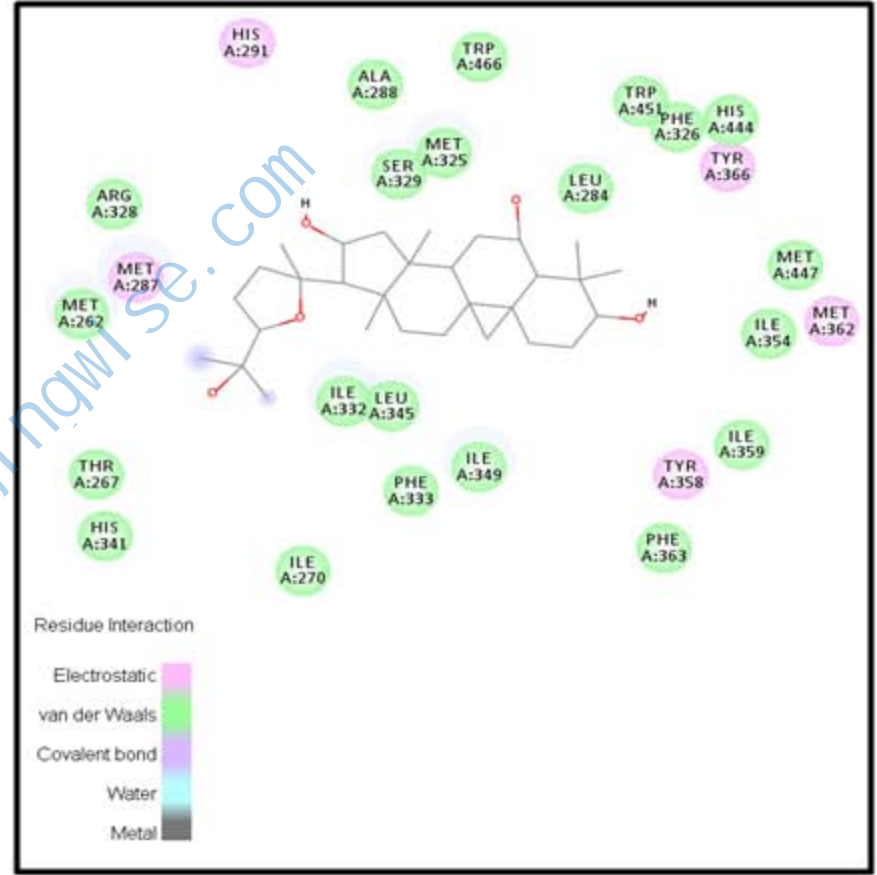
Table 2. Sequences of the mouse primers used in real time PCR

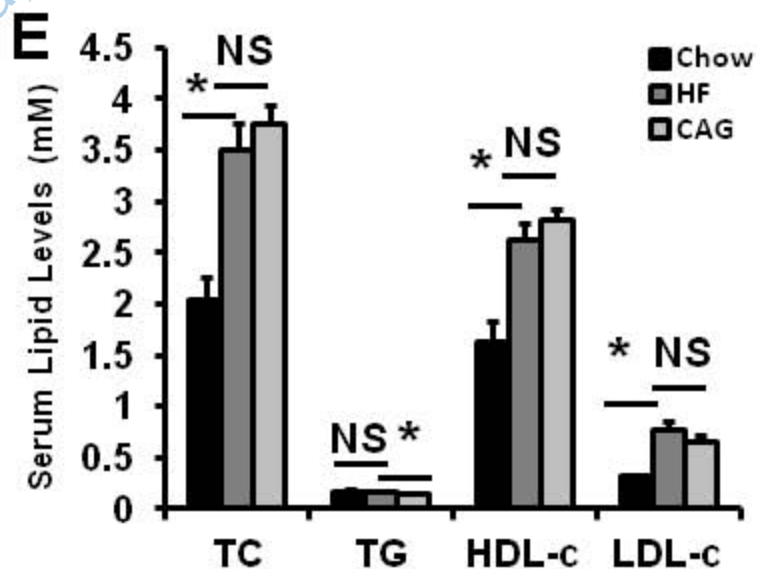
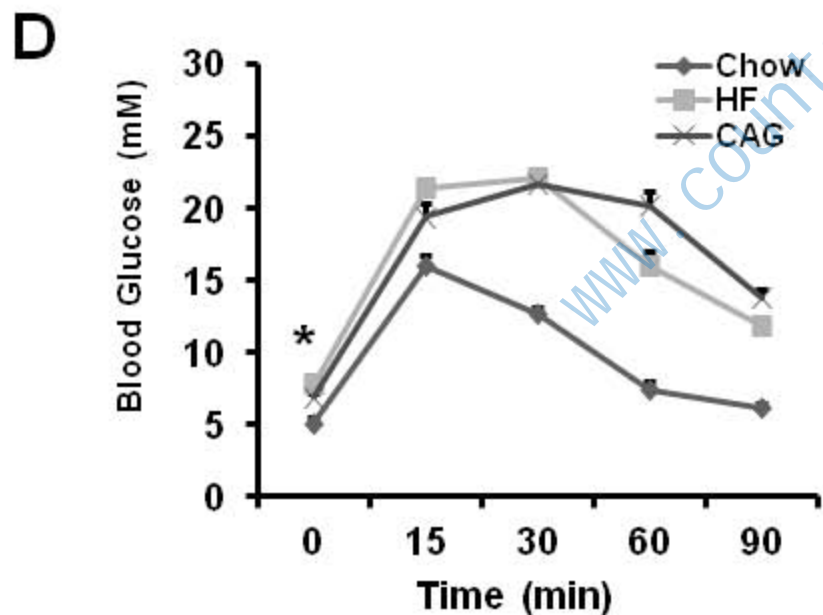
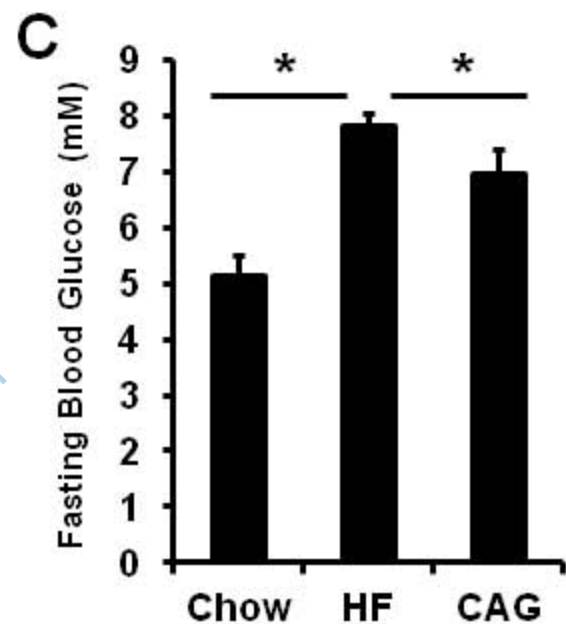
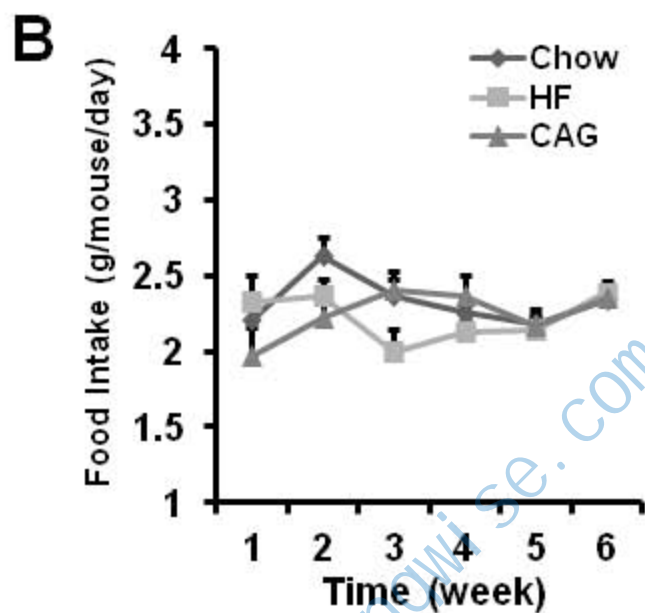
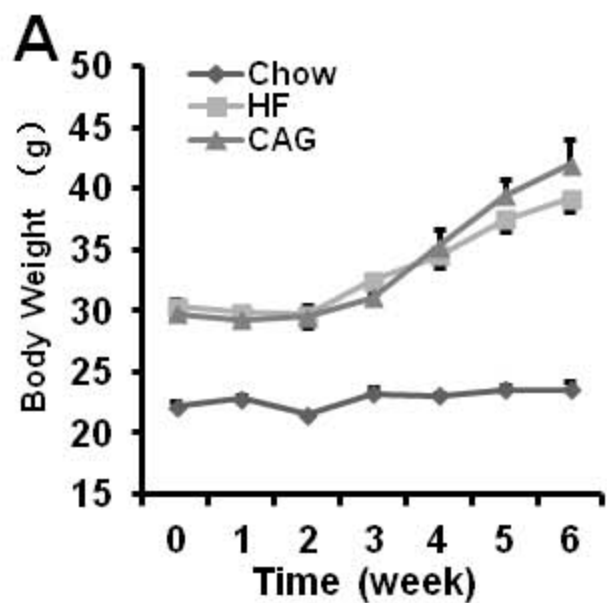
Gene	Sense primer	Anti-sense primer
<i>β-actin</i>	TGTCCACCTTCCAGCAGATGT	AGCTCAGTAACAGTCCGCCTAGA
<i>Nr1h4</i>	TTCCTCAAGTTCAGCCACAG	TCGCCTGAGTTCATAGATGC
<i>Nr0b2</i>	GGAGTCTTTCTGGAGCCTTG	ATCTGGGTTGAAGAGGATCG
<i>Lrh1</i>	TCAGTTCGATCAGCGGGAGTTTGT	TGCAGGTTCTCCAGGTTCTTCACA
<i>Hnf4a</i>	GTGCTTCCGGGCTGGCATGAA	AGGTGATCTGCTGGGACAGAACC
<i>Ppara</i>	AGGCTGTAAAGGCTTCTTTCC	GGCATTGTTCGGTTCTTC
<i>Pparβ</i>	AGTGACCTGGCGCTCTTCAT	CGCAGAATGGTGTCTGGAT
<i>Pparγ</i>	CGCTGATGCACTGCCTATGA	AGAGGTCCACAGAGCTGATTCC
<i>Pgc1a</i>	TGTTCCCGATCACCATATTCC	GGTGTCTGTAGTGGCTTGATTG
<i>Pgc1β</i>	GGGTGCGCCTCCAAGTG	TCTACAGACAGAAGATGTTATGTGAACAC
<i>G6pc</i>	GTGGCAGTGGTCGGAGACT	ACGGGCGTTGTCCAAAC
<i>Pck1</i>	CACCATCACCTCCTGGAAGA	GGGTGCAGAATCTCGAGTTG
<i>Apo2</i>	TGATGTTGGGAAATGAGG	ATCGGGTATGTCTTCTGGTA
<i>Apoai</i>	ACTCGGACTTCTGGGATA	AGTGTCTTCAGGTGGGTTTT
<i>Sult2a1</i>	GAAGTGGCTGATTGAGAT	AGGTTATGAGTCGTGGTC
<i>Scd1</i>	CTTATCATTGCCAACACCA	CTTCTCGGCTTTCAGGTC
<i>Tnfa</i>	ATGGATCTCAAAGACAACCAACTAG	ACGGCAGAGAGGAGGTTGACTT
<i>Mcp-1</i>	AGGTCCCTGTCATGCTTC	GTGCTTGAGGTGGTTGTG
<i>Il1β</i>	TCGTGCTGTCGGACCCATAT	GGTTCTCCTTGTACAAAGCTCATG
<i>Il6</i>	AACCACGGGCTTCCCTACTT	TCTGTTGGGAGTGGTATCCTCTGT
<i>Cyp7a1</i>	TGATCCTCTGGGCATCTCAAGCAA	AGCTCTTGCCAGCACTCTGTAAT
<i>Cyp8b1</i>	GGACAGCCTATCCTTGGTGA	GACGGAACCTCCTGAACAGC
<i>Cyp3a11</i>	AGGCAGAAGGCAAAGAAAGGCAAG	TGAGGGAATCCACGTTCACTCCAA
<i>Osta</i>	CTGATGACAGTGCTGACACG	TTGAGTGCTGAGTCCAGGTC
<i>Ostβ</i>	CTGGCAAACAGAAATCGAAA	TCAAGATGCAGGTCTTCTGG
<i>Ntcp</i>	TATCAGCCCCCTTCAATTC	GTGAGCCTTGATCTTGCTGA
<i>Baat</i>	CCATTGAAAAAGCTCATGGA	ATCAGCTGTGCTATGGCTTG
<i>Bacs</i>	GATGCCCTTGCTACACTCT	AGGACAAGCCCTATCGTAT
<i>Abcb4</i>	CGGCGACTTTGAACTAGGCA	CAGAGTATCGGAACAGTGTCAAC
<i>Abcb11</i>	CGGACCTGTATTGTCATTGC	CCCTTCTGGTCCATCAGTTT
<i>Akr1b7</i>	AAGCGGGAGGATCTCTTCAT	TCAGATCCGAGAGGGTGTTC
<i>Cd68</i>	TCACCTTGACCTGCTCTCTCTAA	GCTGGTAGGTTGATTGTCTGCTG
<i>Cpt1a</i>	TATGTGAGTGAAGTGGTGGGAGGA	TATGGGTTGGGGTGTAGTAGAGC
<i>Cpt1β</i>	TGGGACTGGTCGATTGCATC	CAGGGTTTGTGCGGAAGAAGAAAA
<i>Acox1</i>	CTTGGATGGTAGTCCGGAGA	TGGCTTCGAGTGAGGAAGTT
<i>Fgf15</i>	TGAAGACGATTGCCATCAAG	GAGTAGCGAATCAGCCCGTA
<i>Ibabp</i>	TCACCATTGGCAAAGAATGT	ACCCTCCATCTTCACGGTAG
<i>Asbt</i>	TGACTCGGGAACGATTGTG	GGAATAACAAGAGCAACCAGAGAA

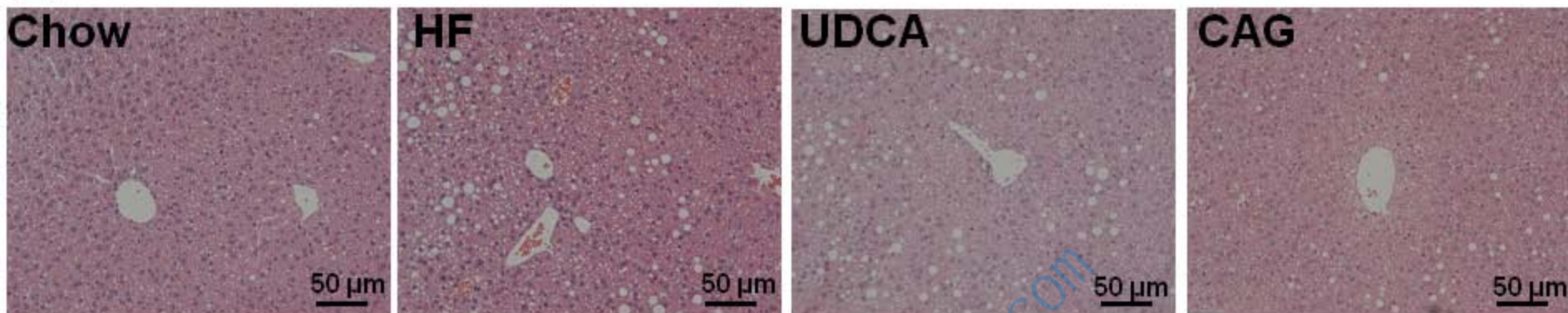
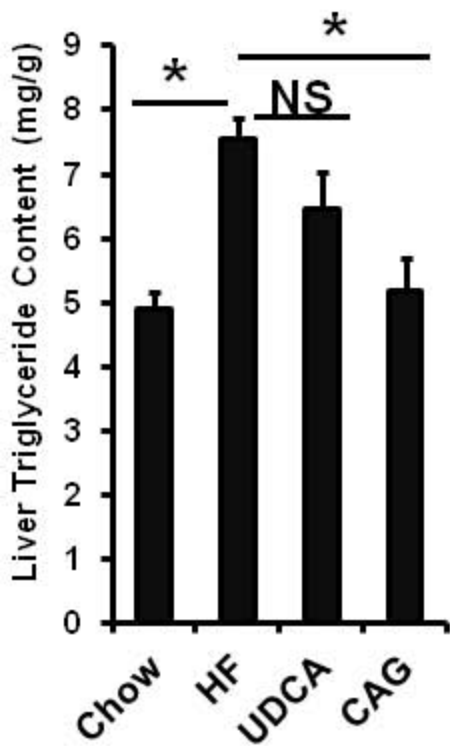
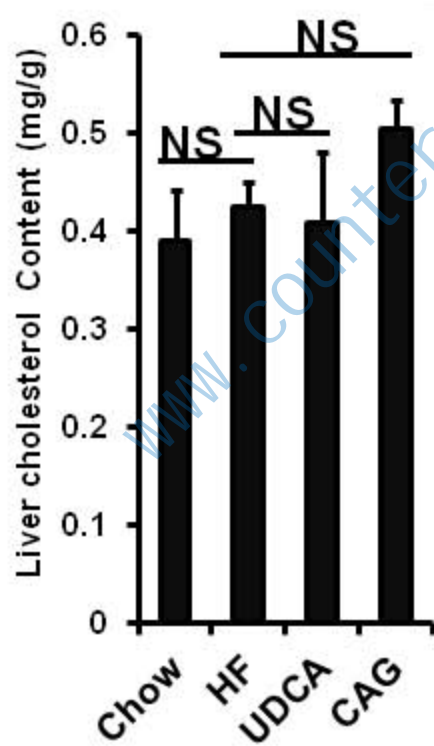
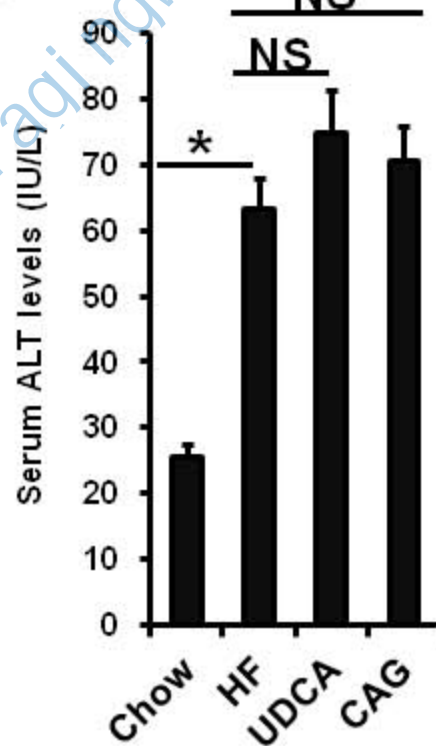
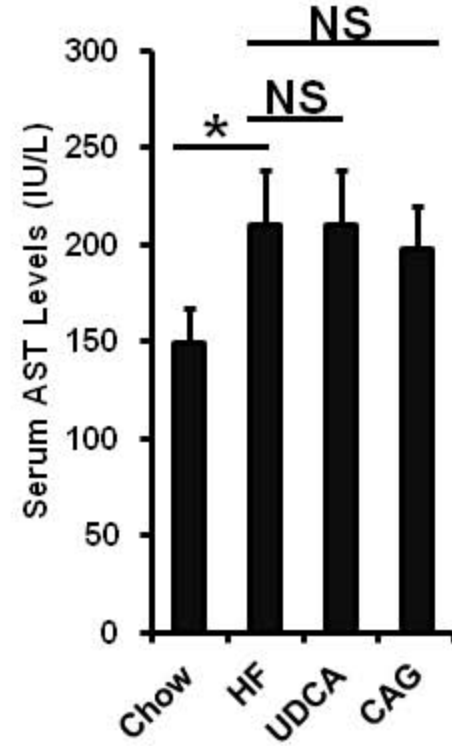
Table 3. Hepatic bile acids composition (%) in DIO mice

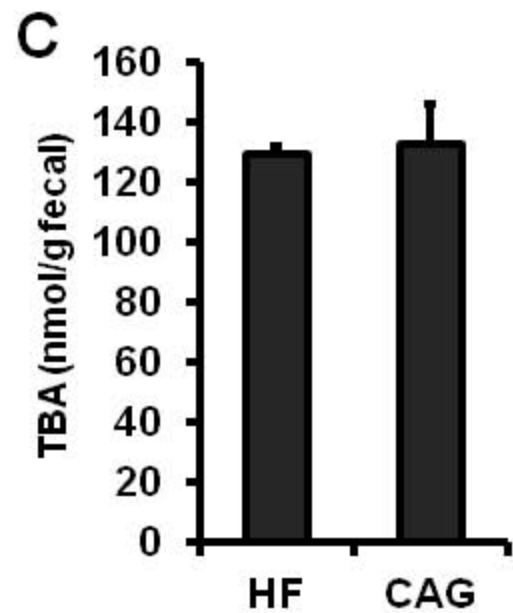
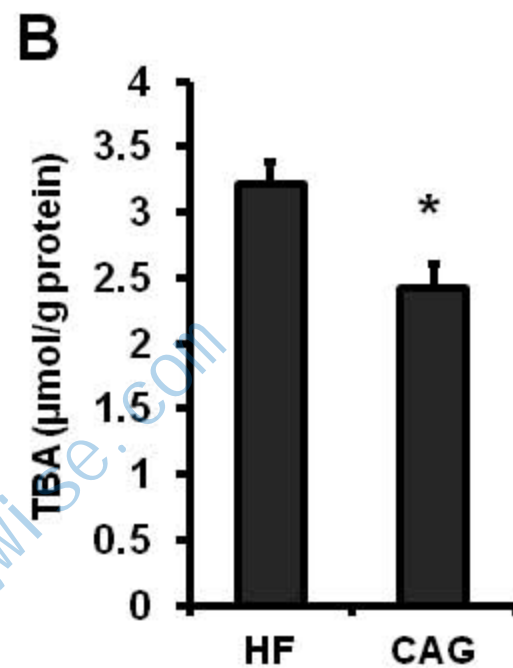
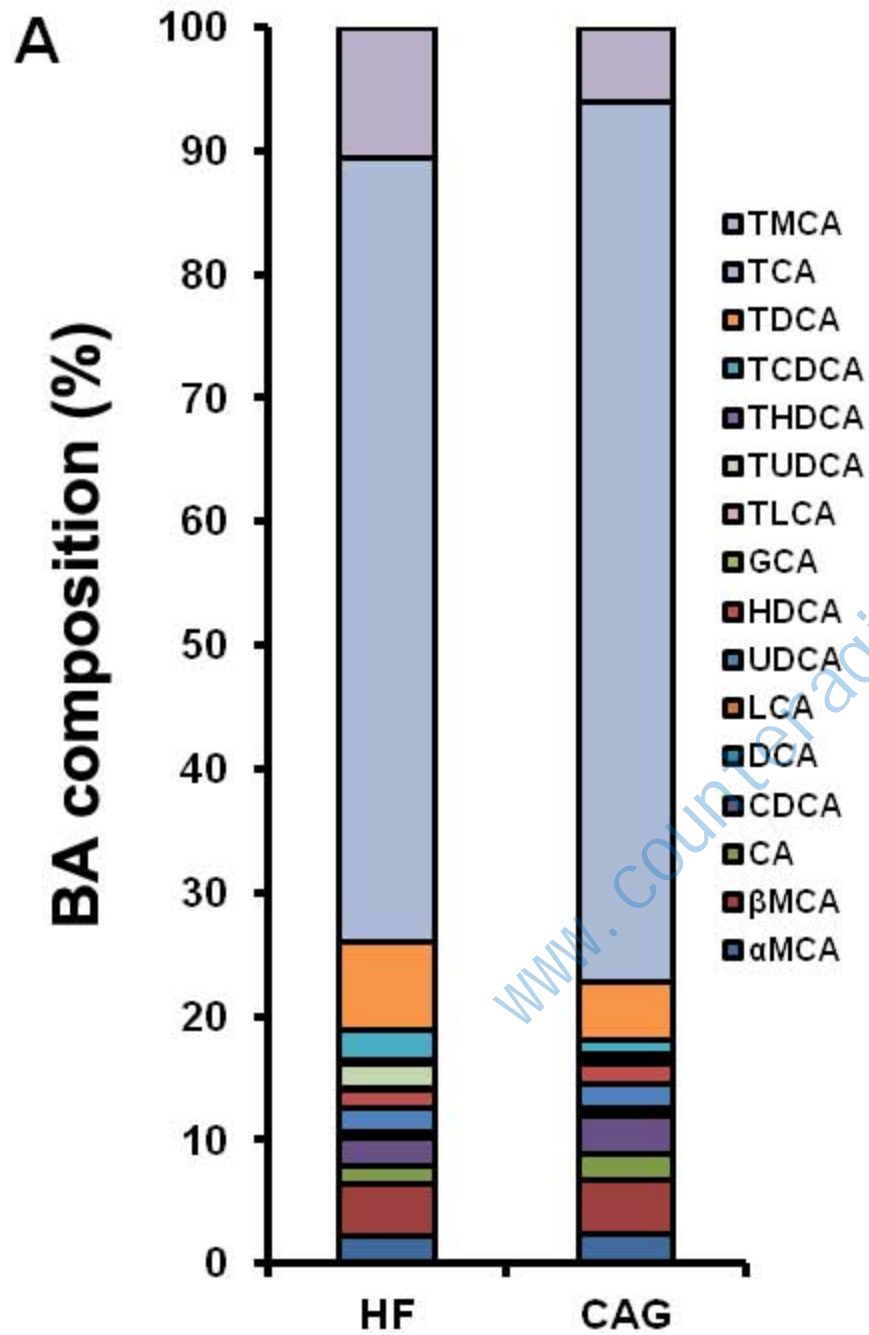
Bile acid	HF	CAG
T-MCA	11.25	5.99
T-CA	67.32	71.41
T-DCA	6.74	4.66
T-CDCA	2.54	1.15
T-HDCA	0.38	0.12
T-UDCA	2.02	0.59
T-LCA	0.09	0.05
GCA	0.04	0.07
HDCA	1.39	1.51
UDCA	2.18	2.03
LCA	0.05	0.17
DCA	0.35	0.38
CDCA	2.44	3.05
CA	1.46	2.19
β MCA	4.04	4.30
α MCA	2.17	2.45

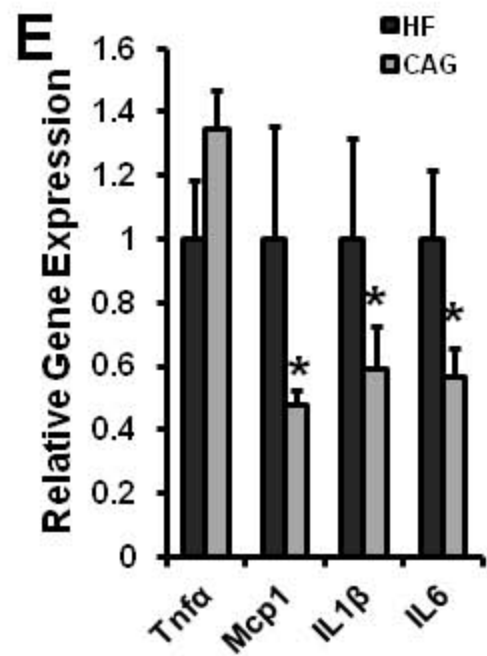
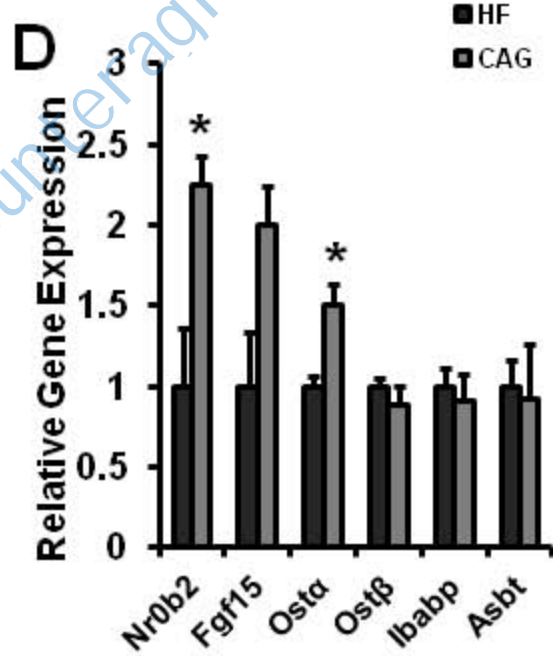
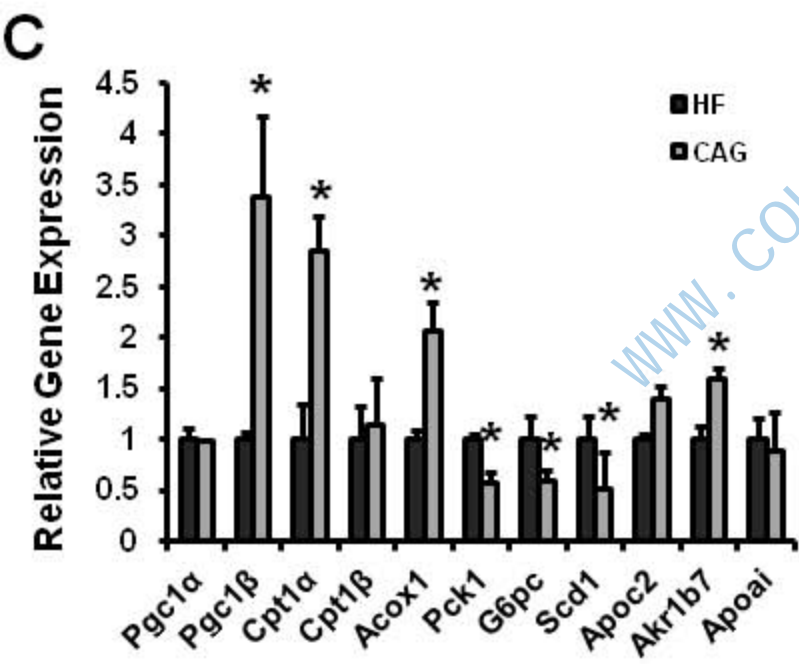
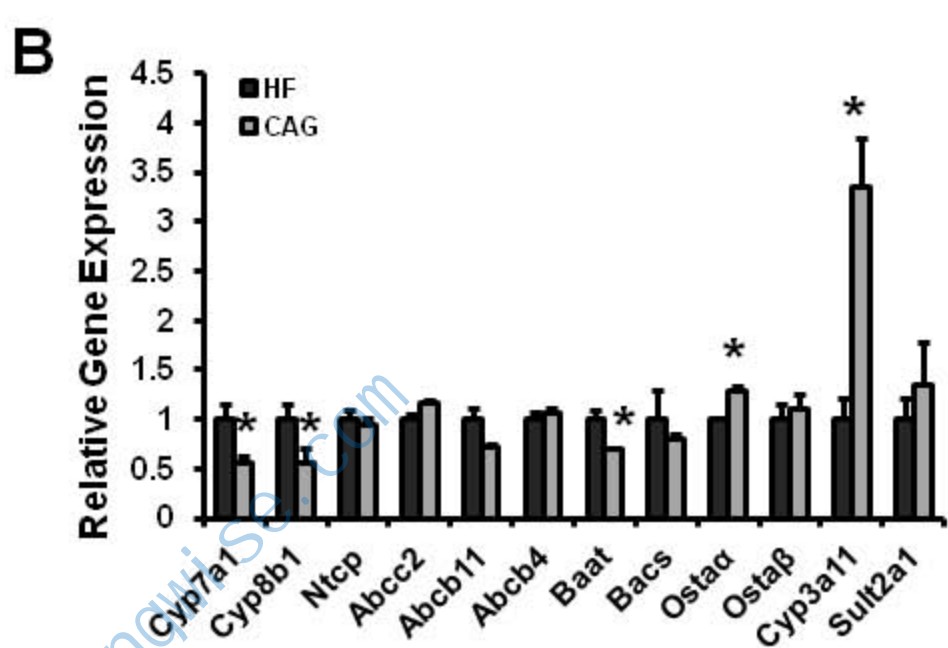
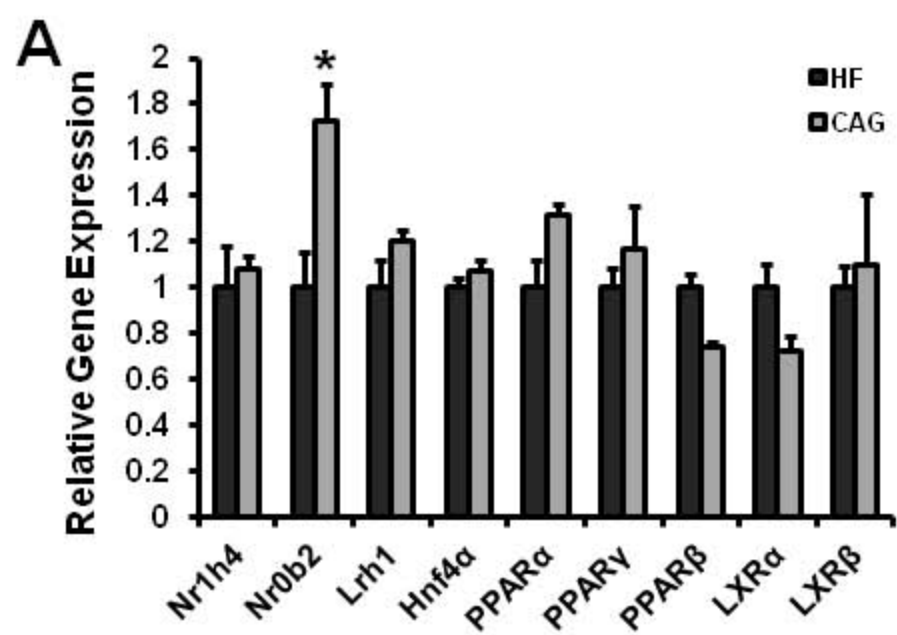
A**B****C****D****E****F****G****H****I**

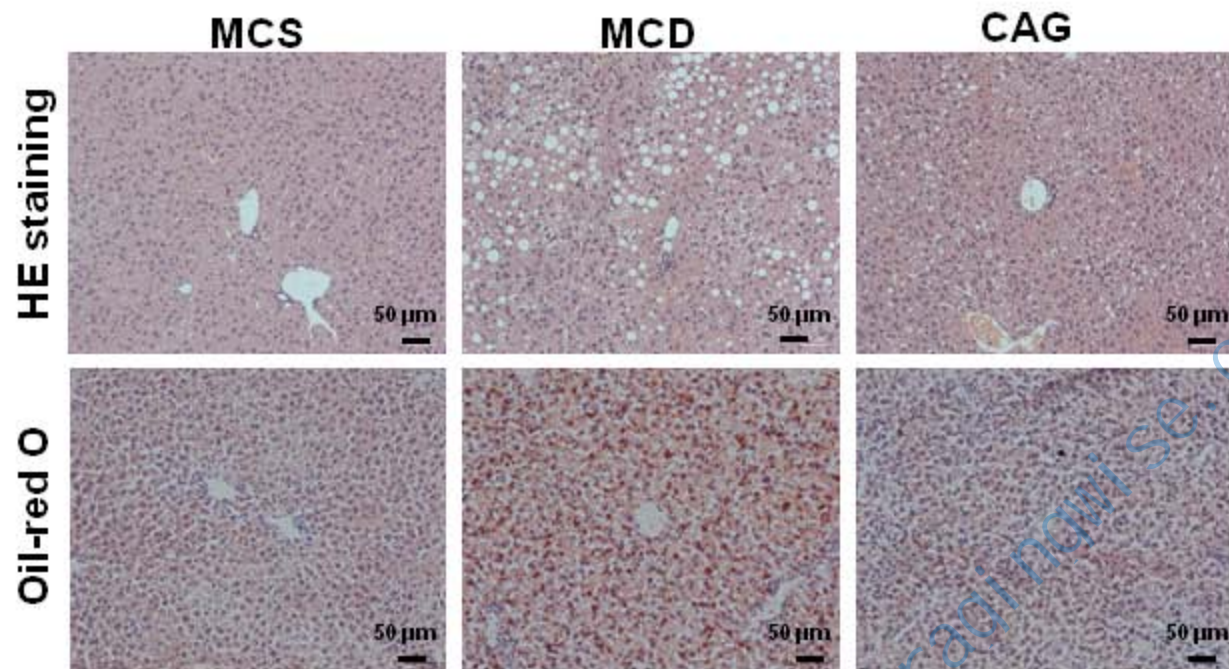
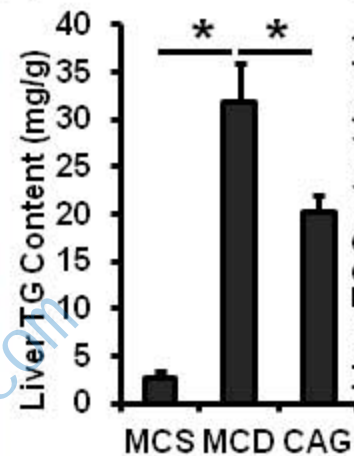
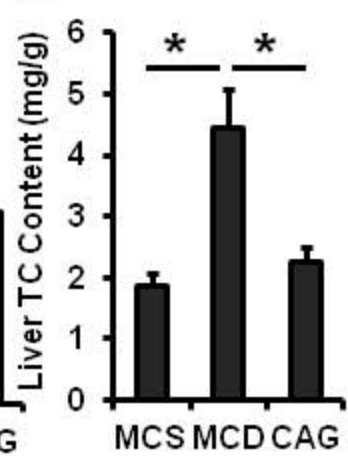
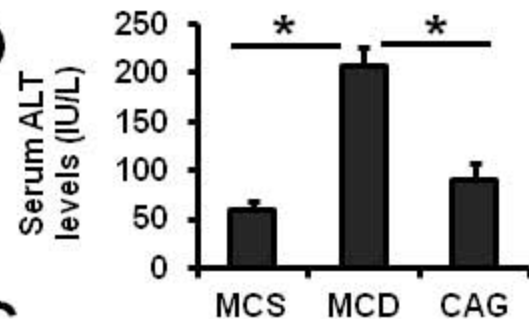
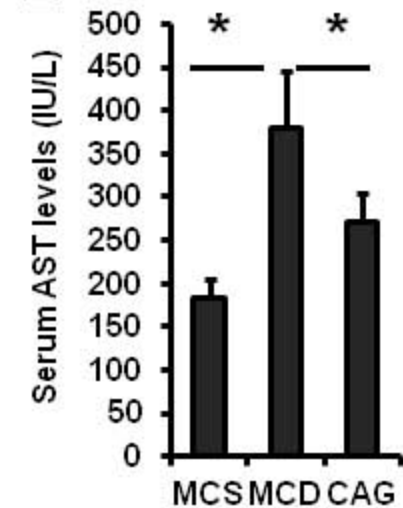
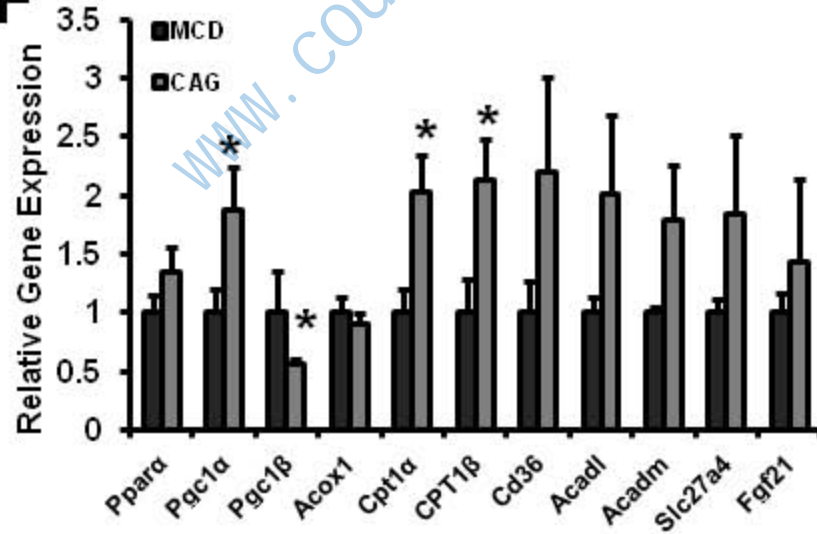
A**B**



A**B****C****D****E**





A**B****C****D****E****F****G**